WORLD CONFERENCE ON TIMBER ENGINEERING
SANTIAGO, CHILE | 24 - 27 AUGUST

DEVELOPMENT OF BEAM TO BEAM CONNECTORS MADE OF DENSIFIED VENEER WOOD

Simon Aurand[1], Hans Joachim Blass[1]

ABSTRACT: In an ongoing research project at KIT Timber Structures and Building Construction an innovative beam to beam connector made of densified veneer wood (DVW) is developed. In a first part of the project different surface modifications were examined aiming at an increased friction between connector and timber member. The modifications included sanding and sandblasting, coating with mineral particles using different bonding agents as well as milling with different milling tools. The static coefficient of friction between the modified densified veneer wood and softwood was determined in tests. Mean friction coefficients greater than 1.0 and characteristic values of up to 0.9 were found. This means a significant increase compared to the value of 0.25 given in Eurocode 5 taking the rope effect into account. In a second part the behaviour of the modified surfaces combined with inclined screws was examined. The positive influence of the surface modification was confirmed. An increase in load-bearing capacity of up to 40% was established. Lastly, a first prototype of a beam to beam connector was manufactured and tested. The results are now used for an improved second prototype.

KEYWORDS: densified veneer wood; DVW; coefficient of friction; system connector; beam to beam connector

1 INTRODUCTION

System connectors are particularly suitable for realizing economical beam to beam connections in timber construction due to their high degree of prefabrication. These connectors are often made of aluminium. However, the high-performance aluminium material has various disadvantages that limit the range of applications for beam to beam connectors. The low fire resistance and the very energy-intensive and expensive production of the aluminium alloys are some of the disadvantages. In a research project at Karlsruhe Institute of Technology (KIT) new connectors made of densified veneer wood (DVW) are developed. The load in such beam to beam connectors is usually transferred with self-tapping screws which are either loaded axially or perpendicular to their axis [1]. In both cases, the contact pressure resulting from the screwing angle activates friction in the shear plane, which increases the load-bearing capacity of the connection. This rope effect is taken into account in Eurocode 5 [2] with a uniform coefficient of friction $\mu = 0.25$ for all interconnected surfaces. The internal forces in the DVW connector are also transferred with inclined screws and are shown schematically in Figure 1. In order to increase the friction in the shear plane between the connector and the softwood member a surface treatment of the DVW is foreseen. This significantly increases the load-bearing capacity of the connection. The focus lies on milled surfaces, as the milling can be easily integrated into the manufacturing process of system connectors.

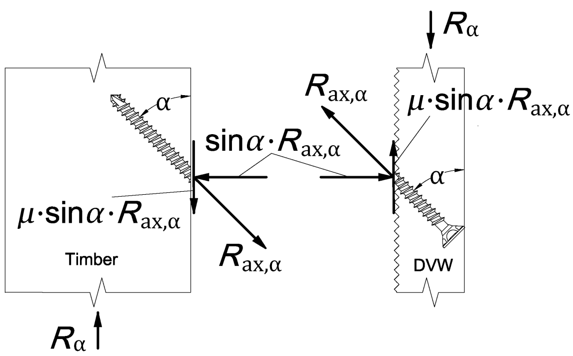

Figure 1: *Internal forces in the shear plane considering friction between the modified surface and the timber member*

2 DENSIFIED VENEER WOOD

DVW consists of stacked beech veneers saturated with thermosetting synthetic resin. The layered veneers are compressed in hydraulic presses under high temperature and high pressure. Because of its very high mechanical properties, electrical insulation properties and chemical resistance DVW is primarily used in the automotive and aviation industries as well as in plant and mechanical engineering. Preferably beech wood is used because it is easy to impregnate, has high strength perpendicular to

[1] Simon Aurand, Timber Structures and Building Construction, Karlsruhe Institute of Technology (KIT), Germany, simon.aurand@kit.edu
Hans Joachim Blass, Timber Structures and Building Construction, Karlsruhe Institute of Technology (KIT), Germany, hans.blass@kit.edu

the grain and is available in sufficient quantities. To quickly and evenly soak the wood structure with synthetic resin mostly thin veneers with thicknesses of 0.4-2.1 mm are used. After stacking the veneers, they are pressed at 100-250 bar and a temperature of 135-165°C until the resins have hardened. This creates panels with a density of up to 1400 kg/m³ [3][4].

In previous experiments the material properties of DVW with cross-layered veneers were determined [5]. Three different thicknesses d = 6 mm, 10 mm and 15 mm were examined. The results as well as corresponding coefficients of variation in parentheses are shown in Table 1. The in-plane bending and tensile strength are almost constant regardless of the thickness, as are the shear strength and the shear modulus. The in-plane compressive strength and the modulus of elasticity both decrease with increasing panel thickness.

Table 1: *Material properties of densified veneer wood depending on its thickness (mean values)*

Material property	6 mm	10 mm	15 mm
Bending strength $f_{m,0,flat}$	113	103	110
(MPa)	(8%)	(7%)	(8%)
Tensile strength $f_{t,0,edge}$	99.4	108	102
(MPa)	(25%)	(13%)	(12%)
Compressive strength $f_{c,0,edge}$	97.2	96.9	80.5
(MPa)	(9%)	(3%)	(10%)
Shear strength $f_{v,0,flat}$	10.1	9.83	9.86
(MPa)	(11%)	(7%)	(8%)
Modulus of elasticity $E_{m,0,flat}$	20300	19500	17600
(MPa)	(8%)	(9%)	(8%)
Modulus of shear $G_{0,flat}$	1200	1400	1400
(MPa)	(8%)	(12%)	(9%)
Density	1363	1376	1381
(kg/m³)	(2%)	(1%)	(1%)
Moisture content	7.1	7.2	6.7
(%)	(13%)	(16%)	(25%)

3 SURFACE TREATMENT

Various types of surface modification of the DVW were examined to increase the friction in the shear plane between the connector and the softwood member and thus to increase the load-bearing capacity of a later connection due to an increased rope effect.

3.1 SMOOTH SURFACE (UNTREATED)

After the pressing process densified veneer wood has a shining top layer, which is very smooth and resembles a lacquered wood or metal surface. In order to create reference values and to quantify the effect of subsequent surface treatments, a first series of tests was carried out with smooth, untreated DVW.

3.2 SANDED

The top layer of the test specimens was sanded using a belt sander and sandpaper with P40 grit. The sanding was carried out transversely to the fibre direction of the top layer and therefore transversely to the load direction during the friction tests. In Figure 2a a noticeable structuring can be seen.

3.3 SANDBLASTED

Each test specimen was sandblasted manually on both sides. As a result, slightly different surfaces appeared on each side and on each test specimen. During the sandblasting, it was observed that the earlywood of the veneers was removed and only the latewood remained. This resulted in a structuring along the fibre direction of the cover veneers and thus parallel to load direction.

3.4 BRUSHED

Both surfaces of the test specimen were brushed with a braided steel wire pot brush. A clear structuring of the surface is visible in Figure 2b but the roughness was hardly noticeable. In preliminary tests only a very low coefficient of friction was determined and therefore this type of surface treatment was not further pursued.

3.5 COATED

Two different bonding agents were used: firstly, a pasty two-component adhesive and secondly, an epoxy resin adhesive tape. The test specimens were coated either with quartz sand with a grain size of 0-2 mm as can be seen in Figure 2c or with grit with a grain size of 2-4 mm. In addition, the test specimens of one test series were coated with skateboard griptape.

3.5.1 Two-component adhesive (2K SE-polymer)

A hybrid system consisting of epoxy resins and silane-terminated polymer was used. The surfaces of the test specimens were sandblasted before the adhesive was applied. A 0.5 mm thick adhesive layer was chosen for coating with quartz sand and a 1.0 mm thick adhesive layer for coating with grit. The test specimens were pressed manually into the respective aggregate. The specimens cured at room temperature for one week, according to the manufacturer's instructions.

3.5.2 Epoxy adhesive tape (EpoxyTape)

Epoxy resin adhesive tapes with an adhesive layer thickness of 1.0 mm and 0.1 mm were used. They were applied at room temperature and then cured in the oven at a temperature of 130°C for 45 min. After the heat treatment cracks were observed along the veneer layers in some test specimens. However, the impact on the mechanical properties was not further investigated. For both thicknesses of adhesive tape only the quartz sand was chosen and pressed with a constant pressure of 2 MPa for two minutes.

3.5.3 Griptape

A commercially available griptape for the top of skateboards for better grip was used. The grain of the griptape was significantly finer than that of the quartz sand and resembled sandpaper. The processing of the grip tape was significantly easier as it already combines adhesive tape and aggregate.

3.6 MILLED

Different patterns were examined by using different milling tools on a CNC milling machine such as a chamfer cutter for longitudinally and transversely arranged grooves or a cartridge mill for circular grooves.

3.6.1 Pyramid pattern

Girardon [6] developed in 2014 form-fitting and rigid connections with milled surfaces. Based on his studies parallel grooves with the same depth were milled into the top layer of the test specimens using a chamfer cutter. The test specimens were then rotated by 90° and again parallel grooves were milled into the top layer resulting in small pyramids. Test specimens with 0.5 mm, 1 mm, 1.5 mm and 2 mm deep grooves were produced. Figure 2d shows an example of a test specimen with pyramids 1.5 mm deep.

3.6.2 Circular pattern

With a cartridge mill circular grooves with multiple intersections were milled 1.0 mm deep into the top layer of the DVW, see Figure 2e. As a result pyramid-like shapes remained at the edge of the test specimen while elongated grooves with a spacing of about 1.5 mm remained in the middle of the test specimen.

3.6.3 Scale pattern

Using a simple end mill that was inclined by 5° longitudinal and transverse grooves were milled 1 mm deep into the surface, similar to the pyramid pattern. This created a scale pattern. Again, preliminary tests resulted in low friction coefficients and therefore this pattern was not further examined.

3.6.4 Embossed pattern

The pyramid pattern was milled into a steel plate using an indexable thread mill. The steel plate was then pressed into the surface of the DVW. The pyramid tips penetrated about 1.0 mm into the top layer and a surface embossed with the impression of the pyramid pattern was created, as can be seen in Figure 2f.

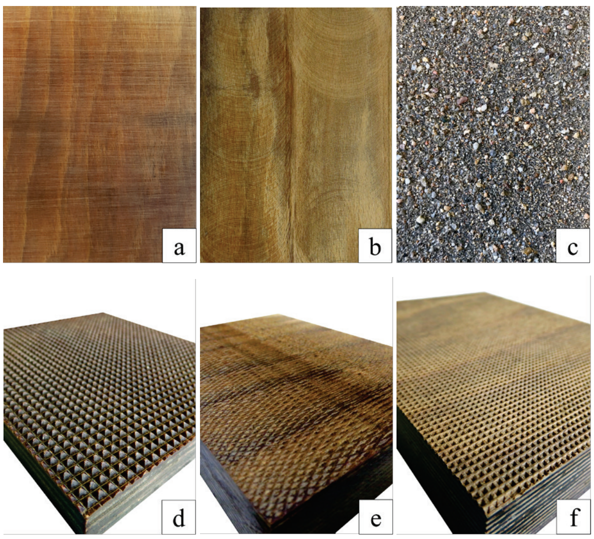

Figure 2: *Some of the examined surfaces: a) sanded, b) brushed, c) coated with quartz sand, d) pyramid pattern, e) circular pattern, f) embossed pattern*

4 COEFFICIENT OF FRICTION

4.1 TEST SETUP

To determine the coefficient of static friction the experimental setup according to Schmidt [7] was used, see Figure 3. The force F_N rectangular to the friction surface was applied with a threaded rod and a spindle. F_N was measured continuously during the tests with a load cell. A calotte between the load cell and the friction surface distributed F_N evenly over the friction surface. The softwood pieces were placed on metal blocks so that the force F_N lies in the centre of the threaded rod and acts centrally on the friction surface. Spruce/fir was used for the softwood, which was stored in a standard climate 20/65 and had an average moisture content of $u = 12\%$. The surfaces were free of knots > 5 mm and without adhesive joints. The force F_{max} parallel to the friction surface was applied using a universal testing machine. The entire test sequence was displacement controlled up to a displacement of 15 mm.

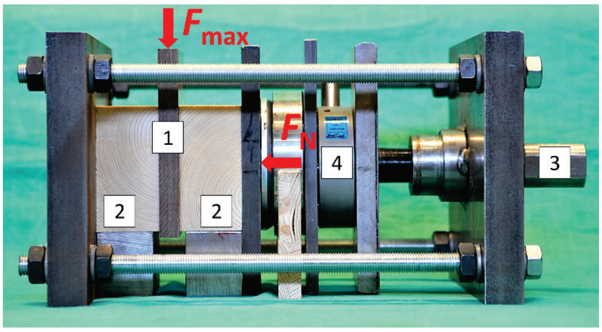

1. DVW specimen with modified surface
2. Softwood specimen
3. Spindle to apply F_N
4. Load cell to measure F_N

Figure 3: *Test setup for friction tests*

During the tests it was distinguished between face grain and end grain of the softwood to cover the different installation situations of the connectors. Contact with the face grain occurs on the main beam, contact with the end grain on the secondary beam. Furthermore, it was distinguished between the grain direction of the side member parallel or perpendicular to the grain direction of the top layer of the DVW or the load direction. The different test configurations can be seen in Figure 4. For the tests side members with a similar density were chosen.

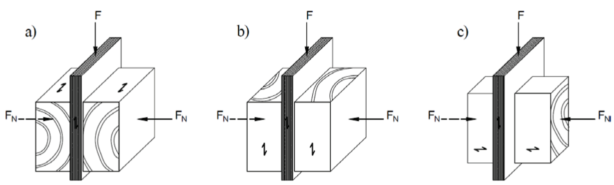

Figure 4: *Friction tests with a) face grain perpendicular and b) parallel to the direction of the load as well as c) end grain*

At the beginning the parameters test speed and normal stress in the friction surface were varied in order to determine the influence of these two parameters. The test speed was varied between 1 mm/min, 5 mm/min and 10 mm/min, the compressive stress perpendicular to the grain between 1 MPa, 2.5 MPa and 6 MPa.

The coefficient of friction is calculated according to equation (1). The force F_{max} is equally divided between the two friction surfaces parallel to the contact surface.

$$\mu = \frac{F_{max}}{2 \cdot F_N} \quad (1)$$

4.2 RESULTS

4.2.1 Evaluation of the parameters contact pressure, test speed and density

The evaluation of the tests with the untreated specimens for which the parameters contact pressure and test speed were changed, show that the friction coefficient is independent of the compressive stress perpendicular to the grain as well as of the test speed. As can be seen in Figure 5 the coefficient of friction remains almost constant with increasing contact pressure and test speed. On the basis of these results for the following tests a compressive stress of 2.5 MPa corresponding to the characteristic compressive strength perpendicular to the grain of softwood was chosen. The test speed was set at 5 mm/min in order to achieve a short test duration of 3 min.

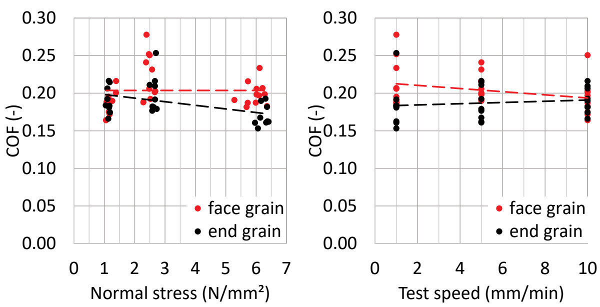

Figure 5: *Impact of the stress perpendicular to the contact area as well as the testing speed on the coefficient of friction*

In addition to the parameters mentioned above the influence of the density of the softwood was examined. Figure 6 shows exemplarily the results for the milled surface with pyramid pattern and the embossed surface. No significant influence of the density on the coefficient of friction can be seen.

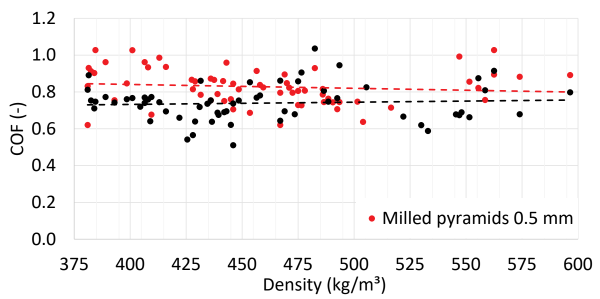

Figure 6: *Influence of the softwood density on the coefficient of friction*

4.2.2 Smooth, sanded and sandblasted surfaces

A clearly pronounced stick-slip behaviour was observed for the tests with unmodified surface and especially for the tests with face grain wood members and low test speed (v = 1 mm/min), as can be seen in Figure 7 on the left. This sudden change of the stick and slip phases can be attributed to two different reasons: on the one hand to the very different stiffnesses of the softwood and DVW in combination with a low test speed and on the other hand to a large difference between static friction and sliding friction coefficients [8]. In comparison the plot for a test with end grain wood members and a test speed of v = 10 mm/min is given on the right in Figure 7.

On average, a coefficient of friction for the smooth surface of $\mu = 0.20 \pm 0.03$ could be determined. For the sanded and sandblasted surfaces more than twice the values were determined with $\mu = 0.56 \pm 0.08$ and $\mu = 0.49 \pm 0.07$ respectively.

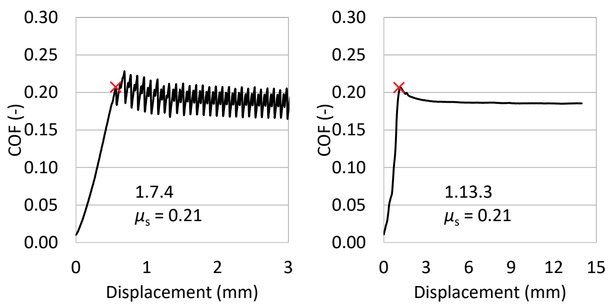

Figure 7: *Exemplary plot for DVW with smooth surface and face grain (left) and end grain (right)*

4.2.3 Coated surfaces

For the test specimens with the two-component adhesive, adhesive failure of the coating could be observed. The glue and aggregate came off the DVW almost completely. This observation was independent of the grain size of the coating. Due to the failure of the adhesive only a lower value of the friction coefficient can be determined. This is $\mu = 0.64 \pm 0.08$ for coating with quartz sand and $\mu = 0.61 \pm 0.05$ for coating with grit. Adhesive failure also occurred when coating with epoxy tape with a layer thickness of 0.1 mm. However, only a few spots of the epoxy tape came off the DVW. During the tests with the epoxy tape with a thickness of 1.0 mm cohesive failure occurred and the aggregate stuck to the softwood. Overall, the results show significantly greater friction coefficients than with the pasty epoxy resin and are on average $\mu = 0.82 \pm 0.10$ for the thin and $\mu = 0.74 \pm 0.03$ for the thick epoxy tape.

For the tests with griptape again no exact coefficient of friction could be determined due to the lack of adhesion of the griptape to the DVW. The average coefficient of friction was $\mu = 0.24 \pm 0.02$ which is only slightly higher than for untreated DVW.

4.2.4 Milled surfaces

For all four examined pyramid patterns the results for the friction coefficients are significantly higher than for the surface treatments shown so far with $\mu = 0.82 \pm 0.11$ (0.5 mm), $\mu = 0.89 \pm 0.10$ (1.0 mm), $\mu = 1.06 \pm 0.11$

(1.5 mm) and μ = 1.15±0.15 (2.0 mm). For the small pyramids with a depth of 0.5 mm the pyramids sheared off parallel to the load direction. Such a damaged surface can be seen in Figure 8a. In addition, severe damage to the softwood surfaces was observed in all tests as can be seen in Figure 8b. The earlywood into which the pyramids were pressed detached itself from the latewood underneath along the annual rings. This was different depending on the annual ring position but was not examined systematically. The larger the pyramids the deeper they pressed into the softwood and the higher the friction coefficients determined.
For the experiments with the circular pattern and the scale pattern, the mean values were calculated to be μ = 0.92±0.12 and μ = 0.66±0.06. The tests with the embossed pattern lead to friction coefficients of μ = 0.79±0.10. The mean values of all the static friction coefficients are given in Table 2.

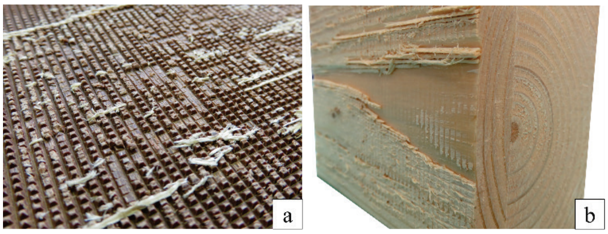

Figure 8: *Damage of a) the pyramid pattern and b) rolling-shear failure of the softwood during friction tests perpendicular to the grain*

4.2.5 Average values and characteristic values

The characteristic values were calculated based on DIN EN 14358 [9] and DIN EN 14545 [10]. For the 5% quantile a global coefficient of variation *COV*g was calculated based on all friction tests. A total of n = 398 friction tests were carried out and the global coefficient of variation *COV*g was calculated to be 0.10.

5 PUSH-OUT TESTS WITH INCLINED SCREWS

Based on the friction tests simple DVW connectors with a modified surface were tested in a first series. The force between the two connector parts was only transferred via pressure contact. The primary objective was to investigate whether inclined screws can generate a sufficiently high contact pressure in the contact area for the previously determined coefficients of static friction to occur. The first connectors were then modified and in series 2 the screws were slightly offset form their original position. To identify the impact, the same screws were used in series 1 and 2. To validate the analytical model in a third series longer screws were used. To investigate the influence of the amount of screws in a fourth series 15 screws were used per connector. And again the same connectors were tested with longer screws. Lastly, a first prototype connector was tested. An overview of the performed tests is given in Table 3.

Table 2: *Summary of determined static coefficients of friction: Mean and characteristic values*

Surface	Coefficient of friction μ Mean value / characteristic value		
	Face grain ⊥	Face grain II	End grain
Smooth	0.20/0.17 n = 31	-	0.19/0.16 n = 27
Sanded	0.56/0.47 n = 6	-	0.47/0.40 n = 6
Sandblasted	0.49/0.41 n = 6	-	0.47/0.40 n = 6
2K SE-polymere and quartz sand	0.64/0.54 n = 3	-	0.54/0.46 n = 3
2K SE-polymere and grit	0.61/0.51 n = 3	-	0.69/0.58 n = 3
EpoxyTape (0.1 mm)	0.82/0.69 n = 3	-	0.97/0.82 n = 3
EpoxyTape (1.0 mm)	0.74/0.62 n = 3	-	0.82/0.69 n = 3
Griptape	0.24/0.20 n = 3	-	0.32/0.27 n = 3
Pyramid pattern 0.5 mm	0.82/0.69 n = 30	0.82/0.69 n = 10	0.84/0.71 n = 20
Pyramid pattern 1.0 mm	0.94/0.79 n = 15	0.88/0.74 n = 20	0.80/0.67 n = 10
Pyramid pattern 1.5 mm	1.06/0.89 n = 20	1.03/0.87 n = 19	1.06/0.89 n = 18
Pyramid pattern 2.0 mm	1.15/0.97 n = 12	-	-
Circular pattern	0.92/0.78 n = 4	-	0.78/0.66 n = 3
Scale pattern	0.66/0.56 n = 7	-	-
Embossed pattern	0.79/0.67 n = 30	0.67/0.56 n = 10	0.71/0.60 n = 21

Table 3: *Tested configurations*

Name	Number of tests	Number of screws	Screw dimensions d x l (mm)
Series 1	3	5	5x100
Series 2	5	5	5x100
Series 3	5	5	6x180
Series 4	5	15	6x100
Series 5	3	15	6x200
Series 6	9	10	6x200

5.1 TEST SETUP AND EXECUTION

The experimental setup is shown in Figure 9. The DVW connectors were only modified on one side and fastened to the side and middle members with inclined screws. Fully threaded screws were chosen for all series.
The test specimens were loaded with a universal testing machine. During the test, both the machine force and the relative displacement between the middle and side members were measured. The relative displacement of each connection was measured on the front and back of the test specimens. The test procedure and the evaluation

were based on DIN EN 26891 [11]. Both the ultimate load $F_{V,test}$ and the stiffness k_s per connector were determined. The stiffness was determined in the range between 10% and 40% of the ultimate load in the linear-elastic range. Three test specimens per surface modification were tested for series 1 and 5 and five specimens per surface for series 2, 3 and 4.

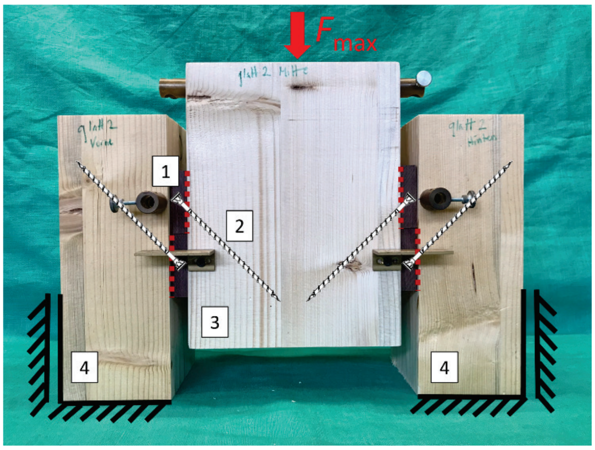

1. DVW connector with modified surface
2. Fully threaded screws inclined by 45°
3. Softwood middle member
4. Softwood side member

Figure 9: *Test setup for the push-out tests with inclined screws*

5.2 RESULTS

The observed types of failure were either a tensile failure of one or more screws in the shear plane or a withdrawal of the screws from the softwood members. Load-displacement plots for series 1 are shown in Figure 10. The results show a significant increase in the load-bearing capacity of the connection for any type of surface modification. The only exception to this are the tests with griptape. As with the friction tests they failed in the adhesive surface. Firstly, tests with untreated surface were carried out in order to determine basic values. The mean value of the maximum load of these tests was $F_{V,test} = 40.5$ kN±0.8 (per connector). Maximum loads of around 53 kN±4.0 could be determined for the different pyramid patterns, which implies a capacity increase of over 30%. Table 4 shows the maximum loads and corresponding stiffnesses for all surfaces examined.

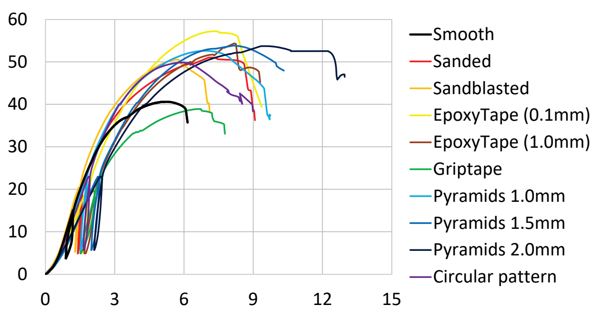

Figure 10: *Force-displacement plots for all tests of series 1 (averaged curves)*

It is noteworthy that with greater pyramid size a higher coefficient of friction is reached and thus a higher load-bearing capacity. However, the greater pyramid sizes lead to lower stiffnesses. In general, it can be stated that higher stiffnesses can be reached with less protruding surfaces.

An inclination of the connectors and impressing of the lower connector edge into the softwood was noticed. Figure 11a shows the connector being pressed into the side member at the lower end and the gapping shear joint at the upper end. In order to avoid the gapping joint in series 2 the screws were offset by a distance *e*. Contrary to expectations the results for the load-bearing capacity are slightly lower.

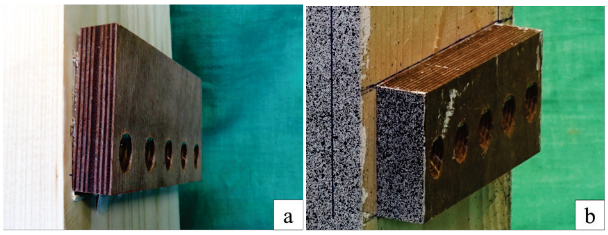

Figure 11: *a) Inclination of the connector and impressing into the softwood and b) no twisting of the connector due to offset screws*

After the tests with five screws similar connectors were tested, however this time with 15 screws. Again, the load between connectors was transferred by compressive stress. Figure 12a shows one of these connectors and the arrangement of the 15 screws. For series 5 for the first time a failure of the DVW itself could be observed. The connector failed to due buckling of the veneers after reaching the compressive strength in the net area. A failed connector can be seen in Figure 12b.

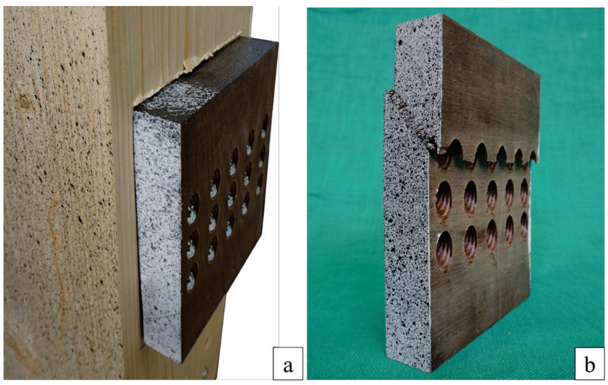

Figure 12: *a) Connector for series 4 and 5 with 15 screws b) failed connector of series 5*

For series 6 a first prototype of a beam to beam connector made of densified veneer wood was manufactured by the industrial partner of this project. Together with the partner, different features were implemented with the key feature being the modified surface. The connector can be seen in Figure 13a. During the tests a mean ultimate load of $F_{V,test} = 151$ kN and a mean stiffness of $k_s = 25.0$ kN/mm was reached. The failure was either due to tensile failure of the screws or compressive failure of the connector itself. After the sudden rupture of all screws on one side tensile failure perpendicular to the grain of either one or both connector plates was observed, see Figure 13b.

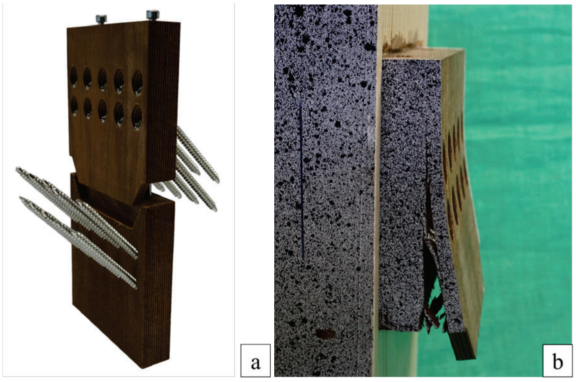

***Figure 13:** a) First prototype of innovative beam to beam connector and b) failed connector after reaching tensile capacity of screws*

***Table 4:** Mean ultimate load and stiffness per connector and comparison ultimate load vs. expected load*

Name	Surface	Capacity (kN)	Stiffness (kN/mm)	Ratio
Series 1 5x100	Smooth	40.5 (2%)	16.7 (5%)	1.11
	Sanded	50.3 (3%)	16.3 (18%)	1.07
	Sandblasted	50.6 (3%)	17.9 (14%)	1.11
	EpoxyTape (0.1 mm)	57.8 (2%)	13.6 (5%)	1.06
	EpoxyTape (1.0 mm)	52.3 (4%)	11.4 (6%)	0.98
	Griptape	39.0 (5%)	11.4 (8%)	1.01
	Pyramids 1.0 mm	52.9 (8%)	15.6 (5%)	0.98
	Pyramids 1.5 mm	53.4 (2%)	12.2 (6%)	0.91
	Pyramids 2.0 mm	52.8 (4%)	11.0 (9%)	0.86
	Circular pattern	49.9 (0%)	14.7 (10%)	1.00
Series 2 5x100 offset	Pyramids 1.0 mm	49.1 (8%)	14.1 (18%)	0.89
	Pyramids 1.5 mm	47.8 (2%)	15.0 (21%)	0.80
Series 3 6x180 offset	Pyramids 0.5 mm	84.5 (6%)	17.8 (7%)	0.92
	Circular pattern	80.0 (3%)	17.7 (10%)	0.89
Series 4 6x100	Pyramids 0.5 mm	153 (3%)	34.0 (18%)	1.05
	Embossed pattern	140 (2%)	42.6 (21%)	1.06
Series 5 6x200	Embossed pattern	185 (6%)	37.4 (10%)	1.00
Series 6 6x200	Pyramids 0.5 mm	151 (3%)	25.0 (16%)	0.82

5.3 EXPECTED LOAD-BEARING CAPACITY

The load-bearing capacity of a connection can be calculated using equation (2). Contrary to Eurocode 5 the effective number of fasteners is set to $n_{\mathrm{ef}} = n$.

$$F_{\mathrm{V,exp}} = n_{\mathrm{ef}} \cdot F_{\mathrm{ax}} \cdot (\cos\alpha + \mu \sin\alpha) \qquad (2)$$

Equation (3) from Blaß et al. [12] determines the withdrawal resistance depending on the screwing angle. The equation is based on over 700 tests and can also be applied to self-tapping screws from other manufacturers, provided the geometric properties are comparable to those of the screws examined.

$$F_{\mathrm{ax}} = \frac{0,6 \cdot \sqrt{d} \cdot \ell_{\mathrm{ef}}^{\,0,9} \cdot \rho^{0,8}}{1,2 \cdot \cos^2\alpha + \sin^2\alpha} \qquad (3)$$

The density of each side and middle member was determined after the tests. For the friction coefficients the mean values from the previous tests were taken. The tensile capacities of the used screws were also determined after the tests and are given in Table 5.

***Table 5:** Tensile capacities of the different screws*

Screw	Capacity (kN)
Fully threaded 5x100 (countersunk head)	8.96±0.06
Fully threaded 6x100 (countersunk head)	15.1±0.43
Fully threaded 6x200 (countersunk head)	14.2±0.10

Head pull-through failure was excluded as tests showed that for 15 mm and 25 mm thick DVW and screws with $d = 6$ mm and a countersunk head only rupture of the screws occurred. Compressive failure of the connector itself was considered with a net area and a compressive strength of $f_{\mathrm{c,0,edge}} = 80.5$ MPa as given in Table 1.
For comparison the ratios of the mean expected loads $F_{\mathrm{V,exp}}$ to the mean ultimate loads from the tests $F_{\mathrm{V,test}}$ were calculated for each test series and are also given in Table 4. The comparison provides a minimum ratio of 0.80 and an average ratio of 0.97. The average ratio of ~ 1 confirms a good alignment of the analytical model with the ultimate loads from the tests, even for significantly higher friction coefficients. Figure 14 further illustrates the comparison $F_{\mathrm{V,test}} / F_{\mathrm{V,exp}}$.

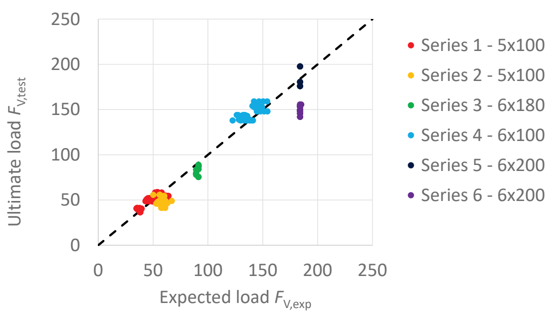

***Figure 14:** Numerical model vs. tests*

5.4 COMPARISON WITH EUROCODE 5

The load-bearing capacity of connections with 45° inclined screws and a coefficient of friction of $\mu = 0.25$ is calculated with Equation (2) to:

$$F_{\mathrm{V,k}} = 1.25 \cdot F_{\mathrm{ax,k}} \big/ \sqrt{2}$$

If, for example, a characteristic friction coefficient of $\mu = 0.80$ for a milled surface with a pyramid pattern is used in Equation (2) the load-bearing capacity is more than 40% higher. Further comparisons of the characteristic load capacities with the value from Eurocode 5 are listed in Table 6.

Table 6: *Increase in characteristic load bearing capacity compared to the Eurocode 5 value of $\mu = 0.25$*

Surface	$\mu_{0.05}$	Face grain ⊥	End grain
Pyramid pattern 0.5 mm	0.70	36%	37%
Pyramid pattern 1.0 mm	0.80	44%	34%
Pyramid pattern 1.5 mm	0.90	52%	52%
Pyramid pattern 2.0 mm	0.97	58%	-
Circular pattern	0.81	45%	33%
Embossed pattern	0.68	34%	28%

6 CONCLUSIONS

The friction tests show that even simple methods of surface modification result in increased friction coefficients between the connector and the wood members. Thus, greater load bearing-capacities can be achieved. The main focus was on the more complexly manufactured milled surfaces which can be easily integrated into the manufacturing process of currently used beam to beam connectors. The characteristic friction coefficients presented in Table 2 mean an increase in the friction coefficient by 2.5 to 4 compared to the value of $\mu = 0.25$ currently specified in Eurocode 5.

However, for the analytical model the static friction values have to be reconsidered, as it is evident, that the displacement in the shear plane between the connector and the softwood at the ultimate load in the push-out tests is mostly greater than the displacement at the maximum friction coefficient in the friction tests. The evaluation of the coefficient of friction has to be adapted to the behaviour of the connectors in the push-out tests. Sample calculations show an even better fit of the analytical model to the test results when the friction coefficients are rather evaluated at certain displacements than at their maximum value.

REFERENCES

[1] Blass, H.J.: Selbstbohrende Schrauben und Systemverbinder – Stand der Technik und Herausforderungen. 23. Internationales Holzbau-Forum, Garmisch-Partenkirchen, 2017.

[2] DIN EN 1995-1-1:2010-12: Eurocode 5: Design of timber structures – Part 1-1: General – Common rules and rules for buildings, Beuth Verlag, Berlin, 2010.

[3] Paulitsch, M. and M.C. Barbu: Holzwerkstoffe der Moderne, DRW-Verlag, Leinfelden-Echterdingen, 2015.

[4] Wagenführ, A. and F. Scholz, editors. Taschenbuch der Holztechnik, 3. Aufl, Carl Hanser Verlag, München, 2018.

[5] Versuchsanstalt für Stahl, Holz und Steine: Prüfbericht Nr. 186147 (unpublished), Holzbau und Baukonstruktionen – Karlsruhe Institute of Technology (KIT), Karlsruhe, 2019.

[6] Girardon, S.: Amélioration des performances mécaniques des assemblages bois sur bois vissés par préparation des interfaces – Application à la réalisation d'éléments de structure (dissertation). Université de Lorraine – École Doctorale RP2E, 2014.

[7] Schmidt, T.: Kontaktverbindungen für aussteifende Scheiben aus Brettsperrholz. Karlsruher Berichte zum Ingenieurholzbau, Bd. 33, KIT Scientific Publishing, Karlsruhe, 2018.

[8] Heslot, F., T. Baumberger, B. Perrin, B. Caroli and C. Caroli: Creep, stick-slip, and dry-friction dynamics: Experiments and a heuristic model. Physical Review E 49(6):4973–4988, 1994.

[9] DIN EN 14358:2016-11: Timber structures – Calculation and verification of characteristic values, Beuth Verlag, Berlin, 2016.

[10] DIN EN 14545:2009-02: Timber structures – Connectors – Requirements, Beuth Verlag, Berlin, 2009.

[11] DIN EN 26891:1991-07: Timber structures; Joints made with mechanical fasteners; General principles for the determination of the strength and deformation characteristics (ISO 6891:1983), Beuth Verlag, Berlin, 1991.

[12] Blass, H.J., I. Bejtka and T. Uibel: Tragfähigkeit von Verbindungen mit selbstbohrenden Holzschrauben mit Vollgewinde. Karlsruher Berichte zum Ingenieurholzbau, Bd. 4, Universitätsverlag Karlsruhe, 2006.